

# INTERNATIONAL SOCIETY FOR SOIL MECHANICS AND GEOTECHNICAL ENGINEERING



*This paper was downloaded from the Online Library of the International Society for Soil Mechanics and Geotechnical Engineering (ISSMGE). The library is available here:*

<https://www.issmge.org/publications/online-library>

*This is an open-access database that archives thousands of papers published under the Auspices of the ISSMGE and maintained by the Innovation and Development Committee of ISSMGE.*

*The paper was published in the proceedings of the 7th International Symposium on Geotechnical Safety and Risk (ISGSR 2019) and was edited by Jianye Ching, Dian-Qing Li and Jie Zhang. The conference was held in Taipei, Taiwan 11-13 December 2019.*

# Probabilistic Assessment of Earth Slopes Subjected to Seismic Load

Jian Ji<sup>1</sup> and Yufeng Gao<sup>1</sup>

<sup>1</sup>Key Laboratory of Ministry of Education for Geomechanics and Embankment Engineering, Hohai University, Nanjing, China, 210098.

E-mail: [ji0003an@e.ntu.edu.sg](mailto:ji0003an@e.ntu.edu.sg)

E-mail: [yfgao1966@163.com](mailto:yfgao1966@163.com)

**Abstract:** This paper examines the seismic stability of earth slopes subjected to rotational failure mode. Permanent displacement is analyzed based on Newmark's sliding block theory, with extension to compute the rotational displacement in the presence of horizontal ground acceleration history. A simplified relationship between the rotational and horizontal motions of a circular failure mass is obtained. By comparing between case studies, the possible reason why this occurs and how the seismic slip surface will differ from the static one is explained. Further discussion is made to the allowable displacement when quantitative judgment of the slope performance is required, which is useful to make a reliability-based design of seismic slope stability.

Keywords: Slope stability; seismic permanent displacement; rotational failure; reliability analysis.

## 1 General Aspects

In designing an engineered slope, geotechnical practitioners are very familiar with the concept of factor of safety ( $F_s$ ) which is the ratio of resisting force (moment) to driving force (overturning moment). The  $F_s$  is a result of limit equilibrium analysis and is easy to understand when the load conditions are static. In the case of seismic load, the ground motion will lead to a temporarily non-limit equilibrium condition, and a certain amount of slope displacement would be induced. Newmark's pioneering work (Newmark 1965) on calculating permanent displacement has achieved noticeable success in the seismic slope stability analysis, as recently reviewed by (Finn 2013). It is recognized that Newmark's sliding block theory is widely used in landslide analysis, where the sliding surface is often very shallow and plane-like. On the other hand, an important challenge of the Newmark's sliding block theory for seismic displacement analysis is that the deep failure mode (with curved sliding surface) which is an important consideration for designing engineered earth slopes, has not been properly dealt with. This type of sliding is of rotational motion, which requires additional computations in relation to the horizontal/vertical ground motion. It is noticed that the latest research interests have been directed to this problem. In dealing with curved sliding surfaces, (You and Michalowski 1999; Massih and Harb 2009) assumed a logspiral rotational mechanism of slope failure to analyze the irreversible displacement caused by horizontal ground shaking. In more general cases, the failure mass is divided into slices or sub-blocks which is similar to the concept of limit equilibrium of slices that commonly adopted in static  $F_s$  calculation, to establish the relationship between rotational and horizontal/vertical ground motions (Shinoda 2015). In order to include more information about the flexibility of the sliding mass, others proposed improved versions of the Newmark's sliding block theory (Makdisi and Seed 1978; Jibson 1993; Kramer and Smith 1997; Bray and Travararou 2007; Rathje and Antonakos 2011; Tsai and Chien 2016).

The Permanent displacement has been well accepted as a useful indicator of seismic slope instability. Nevertheless, it seems difficult to quantitatively judge a slope from safety to failure states. In particular, the allowable displacement,  $D_c$ , a threshold of deformation-based slope instability has not been properly studied. Some others resort to the probabilistic point of view to establish a relationship between the permanent displacement with probability of failure, instead of specifying a unique  $D_c$  for failure identification. (Al-Homoud and Tahtamoni 2000; Bray and Travararou 2007; Jibson and Michael 2009; Strenk and Wartman 2011; Kim and Sitar 2013).

In this study, the seismic stability of earth slopes subjected to deep failure is investigated probabilistically. Firstly, a simple slope stability model based on the Bishop's limit equilibrium method of slices is presented with inclusion of the horizontal ground acceleration. For a slope with a deep rotational failure mode, the permanent rotational displacement is derived from the equations of slice-wise motions. Then, the first-order reliability method is briefly introduced for dealing with uncertainties and computing the probability of failure. At last, parametric studies of a seismic slope stability analysis are conducted, with a probabilistic investigation of the allowable displacement.

## 2 A Seismic Stability Model for Permanent Displacement

*Proceedings of the 7th International Symposium on Geotechnical Safety and Risk (ISGSR)*

*Editors: Jianye Ching, Dian-Qing Li and Jie Zhang*

Copyright © ISGSR 2019 Editors. All rights reserved.

*Published by Research Publishing, Singapore.*

ISBN: 978-981-11-2725-0; doi:10.3850/978-981-11-2725-0\_IS16-6-cd

### 2.1 Rotational permanent displacement

For a soil slope vulnerable to deep seated failure, it is assumed that the sliding mass would have a circular slip surface with rotational geometry ( $x_0, y_0, R$ ). Figure.1 illustrates the displacements of a circular sliding mass (rigid) when a horizontal ground acceleration  $\ddot{u}_b$  is exerted. According to the simplified Bishop method (Nash 1987), the forces acting on a typical slice are also shown in Figure.1.

For the  $i^{\text{th}}$  slice of base angle  $\alpha$  relative to the horizontal, the Mohr-Coulomb mobilized shear strength  $\tau_i = \frac{1}{F_s} [c' + (\sigma_i - p_i) \tan \phi']$ , the normal force  $N_i = \sigma_i l_i$ , and the mobilized shear resistance  $T_i = \tau_i l_i$ , which is written as

$$T_i = \frac{1}{F_s} [c' l_i + (N_i - p_i l_i) \tan \phi'] \quad (1)$$

Resolving vertically, we have

$$N_i \cos \alpha_i + T_i \sin \alpha_i = W_i - (X_{iR} - X_{iL}) \quad (2)$$

The Simplified Bishop method assumes horizontal interslice forces, i.e.,  $X_R = X_L = 0$ . Accordingly, the normal force can be expressed as

$$N_i = \left[ W_i - \frac{1}{F_s} (c' l_i \sin \alpha_i - p_i l_i \tan \phi' \sin \alpha_i) \right] / m_{\alpha_i} \quad (3)$$

where  $m_{\alpha_i} = \cos \alpha_i + \frac{\tan \phi' \sin \alpha_i}{F_s}$

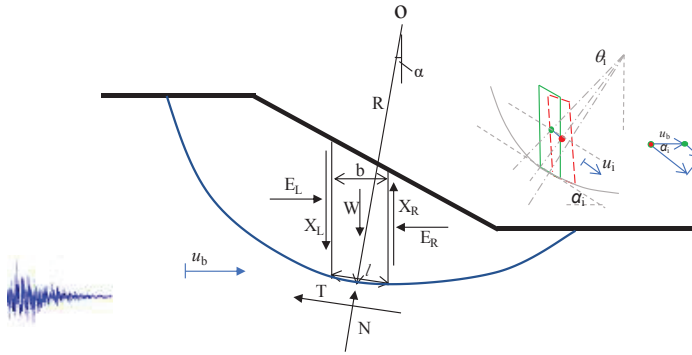


**Figure 1.** Schematics of forces and displacements of a rotational sliding mass based on Bishop simplified method.

For the centre point of slice  $i$  subjected to seismic load, the instantaneous base displacement is  $u_b \cos \alpha$ , the displacement of a slice relative to (i.e., direction parallel to) the sliding base is  $u_{i0}$ , and it can be approximately related to the angular displacement by

$$u_{i0} = \theta \left( R - \frac{h_i}{2} \cos \alpha_i \right) \quad (4)$$

The total displacement of the centre point in the direction of the sliding base is

$$u_i = u_b \cos \alpha_i + \theta \left( R - \frac{h_i}{2} \cos \alpha_i \right) \quad (5)$$

The slice-wise equation of motion along the sliding base can be expressed as

$$E_{iR} \cos \alpha_i - E_{iL} \cos \alpha_i + W_i \sin \alpha_i - T_i = m_i \left[ \ddot{u}_b \cos \alpha_i + \ddot{\theta} \left( R - \frac{h_i}{2} \cos \alpha_i \right) \right] \quad (6)$$

where  $T_i$  is the shear resistance with factor of safety  $F_s = 1$ .

Summing up the equations of motion for all slices will eliminate the interslice forces, and the overall equation of motion is

$$\sum W_i \sin \alpha_i - \sum T_i = \ddot{u}_b \sum m_i \cos \alpha_i + \dot{\theta} \sum m_i \left( R - \frac{h_i}{2} \cos \alpha_i \right) \quad (7)$$

According to Newmark's permanent displacement principle, the permanent displacement will only occur downside, which implies that the rotational displacement is zero at small ground shakings and that it begins to accumulate when the unbalanced seismic force  $F_u$  is greater than zero, i.e.,

$$\begin{cases} \ddot{\theta} = 0, & \text{when } F_u = \sum W_i \sin \alpha_i - \sum T_i - \ddot{u}_b \sum m_i \cos \alpha_i > 0 \\ \ddot{\theta} = \frac{\sum W_i \sin \alpha_i - \sum T_i - \ddot{u}_b \sum m_i \cos \alpha_i}{\sum m_i \left( R - \frac{h_i}{2} \cos \alpha_i \right)}, & \text{otherwise} \end{cases} \quad (8)$$

Over the ground acceleration history, the angular velocity  $\dot{\theta}$  is calculated by integration of Equation 8, and not allowing for negative values:

$$\dot{\theta} = \int \ddot{\theta} dt = \int f(\ddot{u}_b) dt \geq 0 \quad (9)$$

The angular displacement  $\theta$  is therefore:

$$\theta = \int \dot{\theta} dt \quad (10)$$

### 2.2 Critical slip surface under seismic load

The critical slip surface is basically considered to be the worst condition of slope failure, for example, of the smallest factor of safety in a static analysis, or of the smallest seismic coefficient in a pseudostatic analysis. Particularly, a pseudostatic analysis of a rotational slope failure assumes that the moment of equilibrium condition holds during an earthquake shaking. This is obviously not the case as the slope is continuously experiencing displacement, hence no equilibrium condition is applicable.

Following the above solution to rotational permanent displacements, the critical slip surface will be defined to be the one –among a set of predefined ones-- associated to the smallest ground acceleration  $\ddot{u}_b$  when the unbalanced seismic force  $F_u$  is equal to zero, i.e., for all predefined slip surfaces,

$$\min \left( \ddot{u}_b = \frac{\sum W_i \sin \alpha_i - \sum T_i}{\sum m_i \cos \alpha_i} \right) \quad (11)$$

## 3 A Study of Permanent Displacement with Reliability Analysis

### 3.1 First order reliability method

The safety of a slope under a seismic response is evaluated by whether or not the permanent displacement,  $D$ , has exceeded  $D_c$ . The probability of failure is therefore given by:

$$P_f = \text{Prob}(D > D_c) \quad (12)$$

where  $D$  can be obtained by the seismic stability model described in section 2.

From the probabilistic point of view, the statistical information of  $D$  can be derived from the functional combination of all the random variables  $x_i$  under consideration, such that

$$D = D(\mathbf{x}) = D(x_1, x_2, \dots, x_n) \quad (13)$$

The seismic stability model  $D(\mathbf{x})$  involves the integration of the ground acceleration over the time domain based on an (implicit) stability analysis. Therefore, the solution of Eq. (12) can be very complicated and is usually solved using Monte Carlo simulations or by approximate solutions such as first/second-order reliability method (FORM/SORM) (Haldar and Mahadevan 2000). Of interest to this study is the FORM analysis of the permanent displacement, and a limit state function (LSF) is written as

$$g(\mathbf{x}) = D_c - D(x_1, x_2, \dots, x_n) \quad (14)$$

The probability of failure in the framework of FORM is therefore,

$$P_f = \text{Prob}[g(\mathbf{x}) < 0] = \Phi(-\beta) \quad (15)$$

where  $\beta$  is the reliability index defined at the design point (maximum probability point) that can be iteratively solved using an *iHLRF-x* algorithm in the original space of random variables (Ji and Kodikara 2015; Ji et al. 2018). We have:

$$\beta = \sqrt{\left[ \frac{x_i^* - \mu_i^N}{\sigma_i^N} \right]^T \mathbf{R}^{-1} \left[ \frac{x_i^* - \mu_i^N}{\sigma_i^N} \right]} \tag{16}$$

$$\mathbf{x}_{k+1} = \mathbf{x}_k + \lambda_k \mathbf{d}_k \tag{17}$$

$$\mathbf{d}_k = \boldsymbol{\mu}_k^N + \frac{1}{\nabla g(\mathbf{x}_k)^T \mathbf{T}_k \nabla g(\mathbf{x}_k)} \left[ \nabla g(\mathbf{x}_k)^T (\mathbf{x}_k - \boldsymbol{\mu}_k^N) - g(\mathbf{x}_k) \right] \mathbf{T}_k \nabla g(\mathbf{x}_k) - \mathbf{x}_k \tag{18}$$

where  $\mu_i^N$  and  $\sigma_i^N$  are equivalent normal mean and standard deviation of the  $x_i$ , respectively,  $\mathbf{R}$  is the correlation matrix, and  $\mathbf{T}_k = \left[ \sigma_k^N \right]^T \mathbf{R} \left[ \sigma_k^N \right]$ ,  $\lambda_k$  and  $\mathbf{d}_k$  are respectively the step size and search direction defined in the space of original random variables,  $\mathbf{x}$ -space.

**3.2 An illustrative example and parametric analysis**

The seismic stability of the 12 m high cohesive soil slope shown in Figure 2 will be investigated using the proposed method. A porewater pressure coefficient  $r_u = 0.2$  is adopted. One of the well-known El Centro earthquake ground acceleration records (PGA = 0.3g) is selected as horizontal ground motion of the slope model. Since the earth slope is composed of clayey soil, the effect of soil liquefaction due to ground shaking will not be considered in this study.

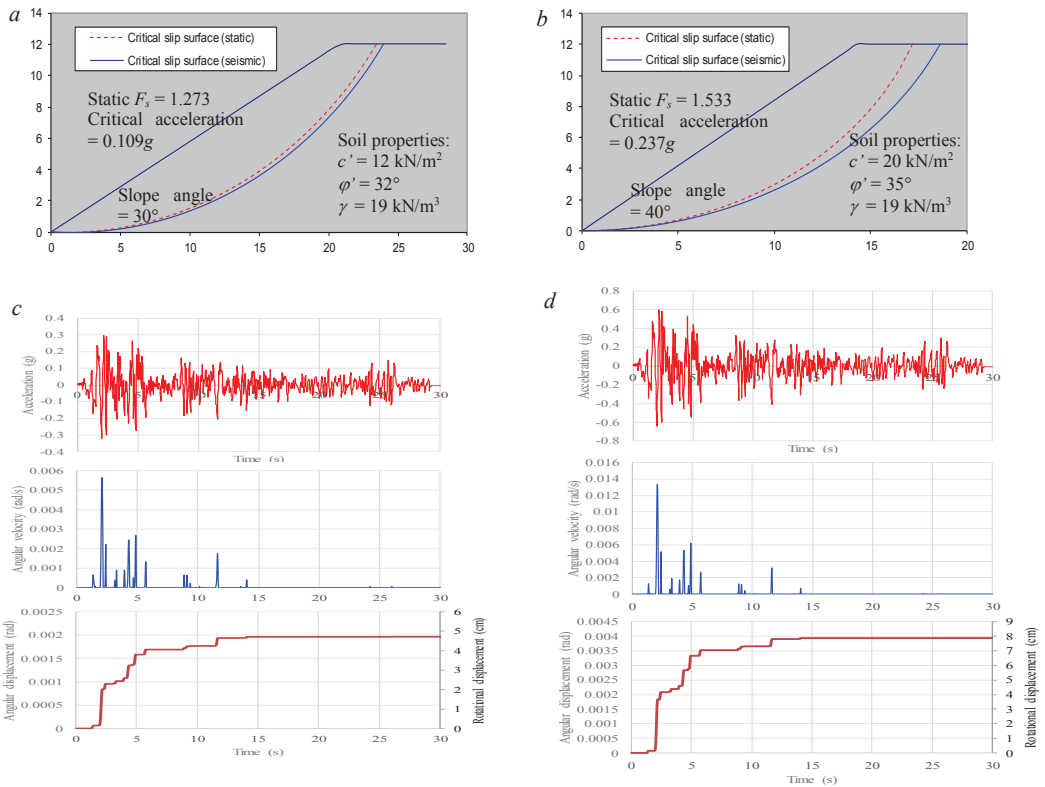


**Figure 2.** Comparison between slope failure modes caused by ground shakings.

**3.2.1 Critical slip surfaces for stability analysis**

In static load conditions, Bishop’s method of slices provided a factor of safety of 1.273, as shown in Figure 2a. This solution was computed using 30 slices and a grid search process to find the static critical slip surface. This homogeneous cohesive soil slope corresponded to a toe failure mode which is as expected from the classical slope stability theory. The same slope model was extended with EL Centro ground acceleration for permanent displacement analysis. In this regard, a grid search for the critical slip surface with respect to minimum

disturbing shaking (i.e., Eq. (11)) was conducted, resulting in a seismic critical slip surface corresponding to a critical ground acceleration of (-)0.109g. Figure 2a compares the subtle difference between them, e.g., the seismic critical slip surface is deeper (and involves more soil mass) than the other.

In Figure 2b, a second slope model was created and analyzed by the same consideration as of Figure 2a. Here the slope has a bigger static factor of safety  $F_s = 1.533$ , and was expected to suffer a stronger earthquake load of  $PGA = 0.6g$ . The difference between static and seismic critical slip surfaces is obviously enlarged. It seems that the more stable the slope is in static condition, the deeper the slip surface would be created by an earthquake. The computed permanent displacements corresponding to Figure 2a and 2b models were presented in Figure 2c and 2d, respectively.

3.2.2 A probabilistic study: reliability index v.s. allowable permanent displacement

Four cases classifying the uncertainty as from very low to high were employed, as listed in Table 1. Note that the mean values are kept the same and standard deviations are changed. They were then used as random variables for a series of reliability computations based on FORM.

Based on the mean values, a small permanent displacement (5.29cm) was obtained when the EL Centro ground acceleration with  $PGA=0.3g$  was considered. By considering various degrees of uncertainties, probabilistic analyses would find the reliability indices (or probabilities of failure), so that the designer can identify the degrees of uncertainty associated to a predefined level of allowable displacement. The probabilistic results are presented in Figure 3. Case 1 was assigned very low uncertainties, with coefficient of variation (COV) of only 0.1 for  $c$  and 0.05 for  $\phi$ . Case 2 was assigned low uncertainties, with a COV of 0.2 for  $\phi$ . Case 3 doubled the COV for  $c$ , and Case 4 was assigned high uncertainties by substantially increasing the COV for both random variables. Obviously, the reliability indices decreased as COV increased for the same threshold of allowable displacement, indicating the seismic stability would be at higher risk of failure for larger uncertainties.

Another interesting observation is, the allowable displacement has played an important role to figure out the reliability index. For example, the results of Case 1 showed that the reliability index increases with allowable displacement dramatically when the latter is relatively small, and becomes insensitive when it is relatively large. The same trend was observed for other cases, although not so clearly as for Case 1. These curves may provide an alternative perspective for the reliability based seismic stability design. For example, the allowable displacement could be justified or back-figured out when information about risk acceptance level (e.g., 5% probability of exceeding the allowable displacement) is available.

Table 1. Four scenarios of soil property uncertainties.

Random variables	Statistical distribution	Random variables	Mean value	Standard deviation
Case 1	Lognormal	$c$	10	1
		$\phi$	28	1.4
Case 2	Lognormal	$c$	10	1
		$\phi$	28	2.8
Case 3	Lognormal	$c$	10	2
		$\phi$	28	2.8
Case 4	Lognormal	$c$	10	3
		$\phi$	28	5.6

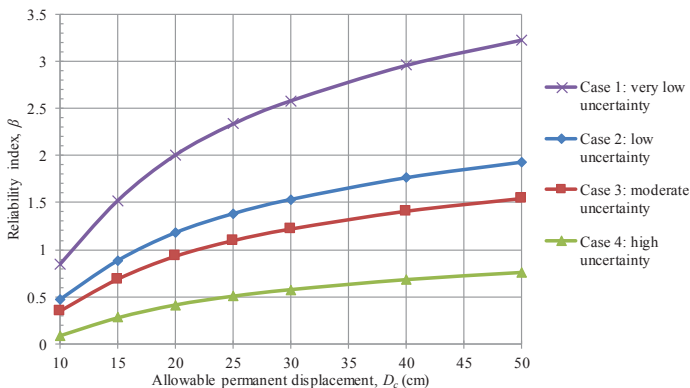


Figure 3. Relationship between reliability index and allowable displacement.

#### 4 Conclusions

This paper proposed a simple framework for seismic slope stability assessment using the Newmark's sliding block theory, as adopted to study the deep failure of earth slopes using Bishop's method. The permanent rotational displacement is obtained by solving the slice-wise equations of motions. Probabilistic analysis was then used to investigate the seismic slope stability and the allowable displacement. Through parametric studies, the following conclusions were drawn:

1. For a slope subjected to seismic load, the potential failure surface differs from that of static load condition, i.e., the factor of safety based critical slip surface. The seismic critical slip surface was shown to be deeper. Although this observation was case specific, it was believed that the ground acceleration providing additional driving forces will cause a larger failure mass to some extent.
2. The degree of uncertainties of soil properties, together with the allowable permanent displacement will lead to the different seismic slope reliability assessment. In particular, it seems that the reliability index increases with allowable displacement dramatically when the latter is relatively small, and becomes insensitive when it is relatively large.
3. The allowable displacement as a threshold for seismic instability judgment can be probabilistically determined if a risk acceptance level (incremental) is available.

#### Acknowledgments

Financial supports from National Science Foundation of China (Grant Nos. 41630638, 51609072, 51879091), and the Fundamental Research Funds for the Central Universities (B18020012) are greatly appreciated.

#### References

- Al-Homoud, A. and Tahtamoni, W. (2000). Reliability analysis of three-dimensional dynamic slope stability and earthquake-induced permanent displacement. *Soil Dynamics and Earthquake Engineering*, 19(2), 91-114.
- Bray, J. D. and Travasarou, T. (2007). Simplified procedure for estimating earthquake-induced deviatoric slope displacements. *Journal of Geotechnical and Geoenvironmental Engineering*, 133(4), 381-392.
- Finn, W. D. L. (2013). Seismic slope stability. *Geo-Congress 2013*, San Diego, California.
- Haldar, A. and Mahadevan, S. (2000). *Probability, Reliability and Statistical Methods in Engineering Design*, New York, Wiley.
- Ji, J. and Kodikara, J. K. (2015). Efficient reliability method for implicit limit state surface with correlated non-Gaussian variables. *International Journal for Numerical and Analytical Methods in Geomechanics*, 39(17), 1898-1911.
- Ji, J., Zhang, C., Gao, Y., and Kodikara, J. (2018). Effect of 2D spatial variability on slope reliability: A simplified FORM analysis. *Geoscience Frontiers*, 9, 1631-1638.
- Jibson, R. W. (1993). Predicting earthquake-induced landslide displacements using Newmark's sliding block analysis. *Transportation Research Record* 1411.
- Jibson, R. W. and Michael, J. A. (2009). *Maps Showing Seismic Landslide Hazards in Anchorage, Alaska*, US Geological Survey.
- Kim, J. M. and Sitar, N. (2013). Probabilistic evaluation of seismically induced permanent deformation of slopes. *Soil Dynamics and Earthquake Engineering*, 44(Supplement C), 67-77.
- Kramer, S. L. and Smith, M. W. (1997). Modified Newmark model for seismic displacements of compliant slopes. *Journal of Geotechnical and Geoenvironmental Engineering*, 123(7), 635-644.
- Makdisi, F. I. and Seed, H. B. (1978). Simplified procedure for estimating dam and embankment earthquake-induced deformations. *Journal of Geotechnical and Geoenvironmental Engineering*, 104(Proceeding), 849-867.
- Massih, D. Y. A. and Harb, J. (2009). Application of reliability analysis on seismic slope stability. *2009 International Conference on Advances in Computational Tools for Engineering Applications*.
- Nash, D., Ed. (1987). Comparative review of limit equilibrium methods of stability analysis. *Slope Stability: Geotechnical Engineering and Geomorphology*, New York, Wiley.
- Newmark, N. M. (1965). Effects of earthquakes on dams and embankments. *Geotechnique*, 15(2), 139-160.
- Rathje, E. M. and Antonakos, G. (2011). A unified model for predicting earthquake-induced sliding displacements of rigid and flexible slopes. *Engineering Geology*, 122(1), 51-60.
- Shinoda, M. (2015). Seismic stability and displacement analyses of earth slopes using non-circular slip surface. *Soils and Foundations*, 55(2), 227-241.
- Strenk, P. M. and Wartman, J. (2011). Uncertainty in seismic slope deformation model predictions. *Engineering Geology*, 122(1-2), 61-72.
- Tsai, C.-C. and Chien, Y.-C. (2016). A general model for predicting the earthquake-induced displacements of shallow and deep slope failures. *Engineering Geology*, 206, 50-59.
- You, L. and Michalowski, R. L. (1999). Displacement charts for slopes subjected to seismic loads. *Computers and Geotechnics*, 25(1), 45-55.